Unconventional spin-density waves in dipolar Fermi gases

S. G. Bhongale, L. Mathey, Shan-Wen Tsai, Charles W. Clark, and Erhai Zhao

Phys. Rev. A **87**, 043604 — Published 5 April 2013

DOI: 10.1103/PhysRevA.87.043604

Unconventional Spin Density Waves in Dipolar Fermi Gases

S. G. Bhongale[1,4], L. Mathey[2], Shan-Wen Tsai[3], Charles W. Clark[4], Erhai Zhao[1,4]
[1] *School of Physics, Astronomy and Computational Sciences, George Mason University, Fairfax, VA 22030*
[2] *Zentrum für Optische Quantentechnologien and Institut für Laserphysik, Universität Hamburg, 22761 Hamburg, Germany*
[3] *Department of Physics and Astronomy, University of California, Riverside, CA 92521*
[4] *Joint Quantum Institute, National Institute of Standards and Technology & University of Maryland, Gaithersburg, MD 20899*
(Dated: March 21, 2013)

We show that unconventional spin order arises naturally in two-component dipolar Fermi gases of atoms or molecules, which recently became accessible experimentally, in optical lattices. Using an unbiased functional renormalization group analysis, we find that dipolar interactions lead to an instability of the gas towards an $\ell = 1$ spin-density-wave state. This phase is the particle-hole analogue of spin-triplet, p-wave Cooper pairs. The order parameter for such spin density waves of p-wave orbital symmetry is a vector in spin space and, moreover, is defined on lattice bonds rather than on lattice sites. We determine the rich quantum phase diagram of dipolar fermions at half-filling on the square lattice as a function of the dipolar orientation, and discuss how these exotic spin density waves emerge amidst competition with superfluid and charge density wave phases.

PACS numbers: 67.85.-d, 75.30.Fv, 71.10.Fd

I. INTRODUCTION

Experiments on ultra-cold atomic and molecular gases have opened new avenues to study many-body physics. One of the central subjects of condensed matter physics is quantum magnetism. A quintessential example is the square-lattice Fermi-Hubbard model at half-filling, which, even at weak coupling, exhibits a spin density wave (SDW) ground state with the well-known checkerboard pattern of spin orientations depicted in Fig. 1(a). Interestingly, the theory of such antiferromagnetic order can be cast analogous to the Bardeen-Cooper-Schrieffer (BCS) theory of s-wave superconductivity – with condensation of particle-hole pairs corresponding to condensation of Cooper pairs in BCS theory [1]. This analogy is quite general and extends to particle-hole condensates with higher angular momenta, predicting the existence of a whole array of SDW states, SDW_ν, where the label $\nu = s, p, d, ..$ indicates angular momentum $\ell = 0, 1, 2, ..$ respectively [1]. The familiar antiferromagnetic order of Fig. 1(a) constitutes SDW_s, whereas SDW_p is the particle-hole analogue of the spin-triplet p-wave superconductors and superfluid ^{3}He [2]. Since superconductors of $p, d, ...$ wave symmetry are commonly referred to as unconventional superconductors, we shall call SDWs with $p, d, ...$ wave symmetry unconventional spin density waves. In the charge sector, a similar analogy predicts the existence of generalized ν-wave charge density waves (CDW_ν) [1].

While several candidate systems have been discussed for spin-singlet charge density waves ($\mathrm{CDW}_{\nu\neq s}$) [1, 3], up to now the realization of spin-triplet $\mathrm{SDW}_{\nu\neq s}$ has remained elusive. The key insight of this paper is that fermions in a 2D lattice with dominant dipole-dipole interaction have the right ingredients to stabilize p- and d-wave SDWs. Before presenting our theoretical evidence for their existence, here we first outline the main features of these unconventional SDWs. These exotic states display a modulation of spin vector $\boldsymbol{\mathcal{S}}$ defined on the bonds of the lattice, such as the checkerboard pattern of red arrows depicted in Figs. 1(c) and 1(d), as opposed to modulation of on-site spin density in conventional SDW_s shown in Figs. 1(a). Specifically, the order parameter of SDW_p, featuring particle-hole pairs with p_y-orbital symmetry, is related to $\mathcal{S}^\eta = \sum_{\alpha,\beta}\langle\hat{a}^\dagger_{i,\alpha}\hat{\sigma}^\eta_{\alpha\beta}\hat{a}_{j,\beta}\rangle$ for relative coordinate $\mathbf{r}_i - \mathbf{r}_j = \hat{y}$ (all distances are in units of the lattice constant throughout this paper). Here $\hat{\sigma}^\eta$ with $\eta \in \{x, y, z\}$ are the Pauli matrices, and $\hat{a}^{(\dagger)}_{i,\alpha}$ is the fermionic annihilation (creation) operator for pseudo-spin $\alpha \in \{\uparrow, \downarrow\}$ at site i. The SDW_{s+d} shown in Fig. 1(d) contains an extended s-wave and a d_{xy} wave component, and its order parameter is defined similarly with (i, j) corresponding to diagonally opposite sites, e.g., $\mathbf{r}_i - \mathbf{r}_j = \hat{x} + \hat{y}$. In contrast, the conventional SDW_s and CDW_s are described by on-site order parameters $\sum_{\alpha,\beta}\langle\hat{a}^\dagger_{i,\alpha}\hat{\sigma}^\eta_{\alpha\beta}\hat{a}_{i,\beta}\rangle$ and $\langle\hat{n}_i\rangle = \sum_\alpha\langle\hat{n}_{i,\alpha}\rangle = \sum_\alpha\langle\hat{a}^\dagger_{i,\alpha}\hat{a}_{i,\alpha}\rangle$ respectively.

The main purpose of this paper is to demonstrate that SDW_p and SDW_{s+d} emerge between two familiar phases of matter, CDW and the BCS superfluid, in the phase diagram of dipolar fermions on a square lattice as the direction of the dipoles is continuously tuned. This results from the competition among the short-ranged on-site interaction and the anisotropic long-ranged dipolar interactions.

II. DIPOLAR FERMIONS IN A LATTICE

In a new generation of experiments, ultra-cold gases of dipolar fermions have become accessible in the quantum degenerate limit. Fermionic atoms of dysprosium 161, with a large magnetic moment of 10 Bohr magneton, have been successfully trapped and cooled well below quantum degeneracy [4]. The fermionic polar molecule $^{40}\mathrm{K}^{87}\mathrm{Rb}$ has been cooled near quantum degeneracy [5] and loaded

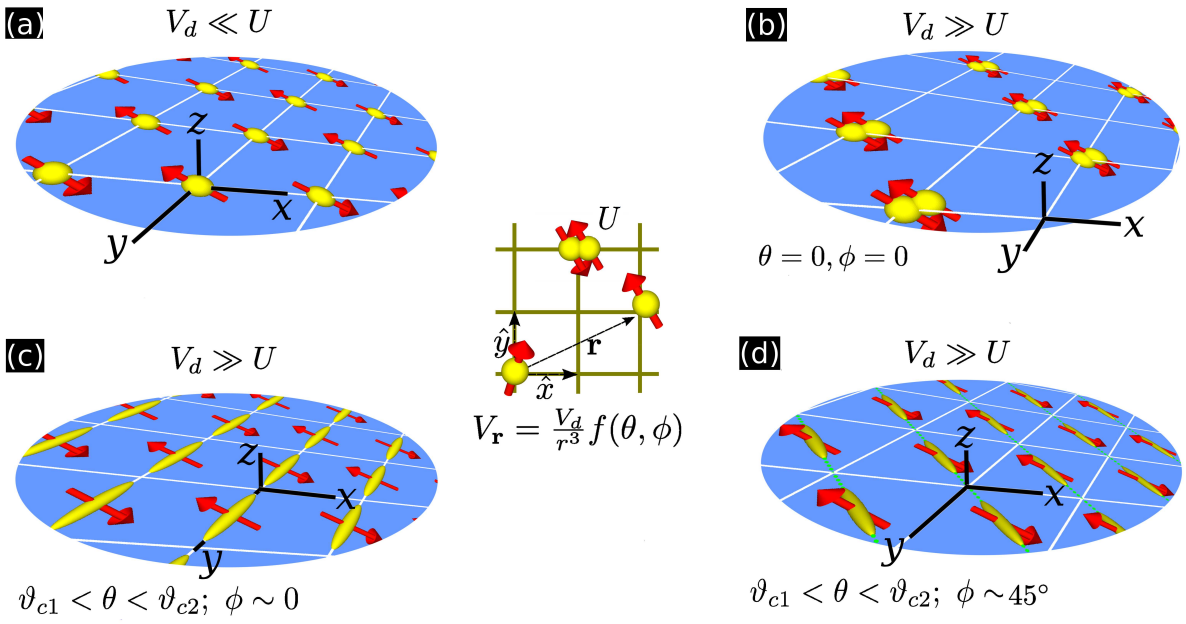

FIG. 1: Schematic spin and charge order for pseudo-spin 1/2 dipolar fermions in two dimensions. The central image illustrates the onsite interaction U between opposite spins (red arrows) and the dipolar interaction $V_{\mathbf{r}}$, here assumed to be spin-independent. The characteristic scale for $V_{\mathbf{r}}$ is $V_d = d^2/a^3$, with a the lattice spacing. $V_{\mathbf{r}}$ depends also sensitively on the orientation of the dipoles labelled by angles (θ, ϕ). (a) The conventional antiferromagnetic spin density wave (SDW$_s$). (b) Checkerboard charge density wave (CDW$_s$), where "charge" is defined as the total density. (c) An example of p-wave spin density waves (SDW$_p$) with modulation of y bond variables. (d) An example of mixed (extended) s- and d-wave spin density waves (SDW$_{s+d}$). Red arrows in (c) and (d) indicate the direction of the spin vector $\boldsymbol{\mathcal{S}}$ defined on the bonds (yellow ellipsoids).

into optical lattices [6]. Recently, the formation of ultracold fermionic Feshbach molecules of ^{23}Na^{40}K has been achieved [7]. On the theory side, many body physics of single-species (spinless) dipolar Fermi gases have been explored by many groups. Numerous quantum phases are predicted: charge density wave [8–11], p-wave superfluid [12–16], liquid crystalline [17–19], supersolid [22], and bond-order solid [3].

Here we consider a two-component (pseudo-spin 1/2) dipolar Fermi gas [23–25] in an optical square lattice at half filling. The two pseudo-spin states can be two hyperfine states of Dy atoms, or two rovibrational states of KRb molecules. This provides a tunable platform for quantum simulation of interacting fermions with long-range interactions [20, 21], beyond the Fermi-Hubbard model. The system is described by the Hamiltonian

$$\hat{H} = -\sum_{\langle i,j\rangle,\sigma} t\hat{a}^\dagger_{j,\sigma}\hat{a}_{i,\sigma} + \frac{U}{2}\sum_{i,\sigma}\hat{n}_{i,\sigma}\hat{n}_{i,-\sigma} + \sum_{i\neq j} V_{ij}\hat{n}_i\hat{n}_j. \quad (1)$$

The lattice is aligned along the x- and y-directions, with nearest neighbor hopping t and on-site interaction U. U contains contributions from the bare short range interaction, and the on-site dipolar interaction $V^\perp_{ii}$, defined below. We assume that all dipoles are aligned in the same direction $\mathbf{d} = d\hat{d} = (d, \theta, \phi)$ by an external magnetic (or electric) field. In general, the off-site dipole-dipole interaction can be decomposed into equal- and unequal-spin components, labeled by $\parallel$ and $\perp$, respectively, $V^\parallel_{ij}\hat{n}_{i\sigma}\hat{n}_{j,\sigma} + V^\perp_{ij}\hat{n}_{i\sigma}\hat{n}_{j,-\sigma}$, and depends on $\hat{d}$ and $\mathbf{r} = \mathbf{r}_i - \mathbf{r}_j$ via $V^{\parallel(\perp)}_{\mathbf{r}}(\hat{d}) \equiv V^{\parallel(\perp)}_{ij}(\hat{d}) = \langle ij|V^{\parallel(\perp)}_{dd}(\hat{d})|ij\rangle = V^{\parallel(\perp)}_d[1 - 3(\hat{r}\cdot\hat{d})^2]/r^3$. We will mostly assume $V^\perp_d(\hat{d}) = V^\parallel_d(\hat{d}) \equiv V_d(\hat{d})$, as in Eq. 1, which arises naturally when the two states are associated with the same hyperfine manifold. The $V^\perp_d(\hat{d}) \neq V^\parallel_d(\hat{d})$ case will be discussed briefly in Section III.C.

To give a heuristic argument about possible orders of the system, we first consider a simplified version of model (1) retaining only the nearest and next-nearest neighbor dipolar interactions, denoted $V_{\hat{x}(\hat{y})}$ and $V_{\hat{x}+\hat{y}}$ respectively, see Fig. 1. First, for $\hat{d} = \hat{z}$, dipolar interactions are purely repulsive. For $U \gg V_d$, the Hamiltonian reduces to the Fermi-Hubbard model, implying a ground state with SDW$_s$ order at half-filling, Fig. 1(a). For $U \ll V_d$, the dipolar energy is reduced by placing same-spins on diagonally opposite sites, while opposite spins share the same site with only a small energy cost U. This implies a checkerboard modulation of the total density $n_i = \langle\hat{n}_i\rangle$, *i.e.* CDW$_s$, shown in Fig. 1(b).

As $\hat{d}$ is tilted away from $\hat{z}$ towards the $\hat{x}$-direction, there exists a region of tilting direction for which the nearest neighbor interaction $V_{\hat{x}}$ becomes attractive while $V_{\hat{y}}$ and $V_{\hat{x}+\hat{y}}$ remain repulsive. For instance, for $\phi = 0$, this region is bounded by two critical values of θ: $\vartheta_{c1} =$

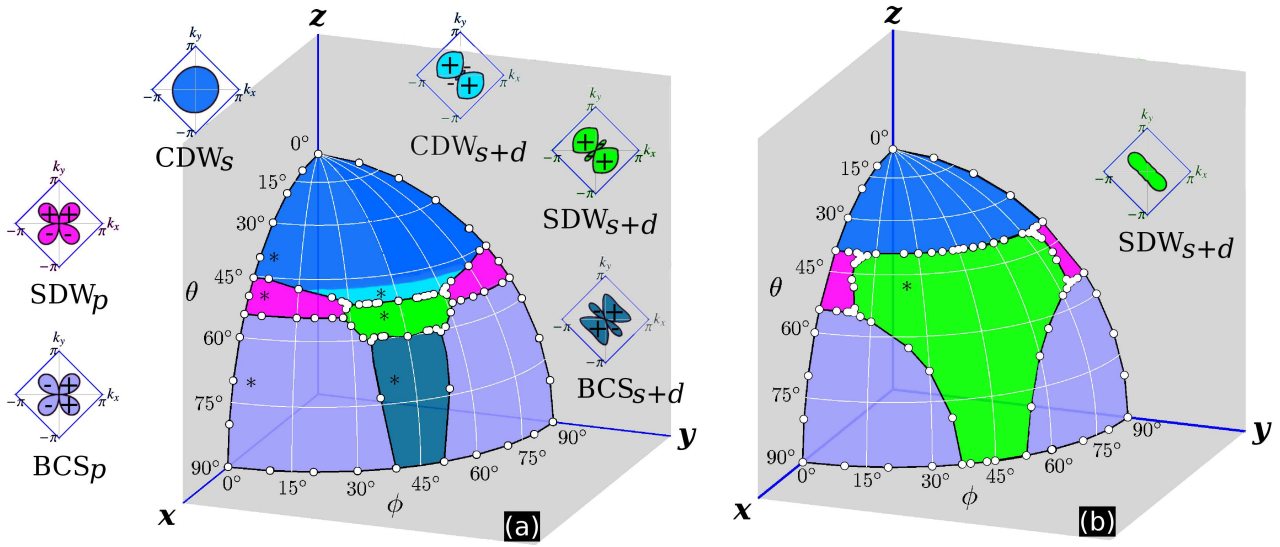

FIG. 2: Phase diagram of dipolar fermions on a square lattice at half filling obtained from FRG. It is shown on the surface of a sphere as a function of the dipole orientation angle θ and ϕ for fixed interactions (a) $V_d = 0.5, U = 0.1$; and (b) $V_d = 0.5, U = 0.5$ in units of t. Unconventional SDWs (SDW$_p$ and SDW$_{s+d}$) are sandwiched between the CDW and BCS superfluid phase. The FRG eigenwavefunction corresponding to a representative point (marked by "$*$") in each phase is shown in the $k_x - k_y$ polar plots with matching colors. Note that FRG predicts a mixed $s + d$-wave (rather than pure d-wave) SDW. As the on-site interaction is increased from $U = 0.1$ in (a) to $U = 0.5$ in (b), the SDW$_{s+d}$ phase expands and squeezes out the neighboring phases. The s-wave component of SDW$_{s+d}$ increases with U, while the d-wave component diminishes.

$\cos^{-1}(\sqrt{2/3}) \approx 35^\circ$ and $\vartheta_{c2} = \sin^{-1}(\sqrt{2/3}) \approx 54^\circ$. In the simpler case of spinless dipolar fermions, a checkerboard bond order solid is formed in this region [3]. Then it is plausible that for the spin 1/2 case, unconventional SDWs of non-s wave symmetry may be stabilized by interaction-induced correlated hopping either along the $\hat{x}$, $\hat{y}$, or the diagonal $\hat{x} + \hat{y}$ direction. The spatial symmetry of these SDWs depends on the value of ϕ. This scenario is illustrated in Figs. 1(c) and 1(d).

Finally, for large dipole tilting angles, *e.g.*, $\theta > \vartheta_{c2}$ for $\phi = 0$, the dominant dipolar interaction is attractive. The leading instability is towards formation of Cooper pairs. Again, the precise orbital symmetry of the BCS phase is determined by the value of ϕ.

III. PHASE DIAGRAM

A. Functional Renormalization Group analysis

We now determine the phase diagram in the weak coupling limit, $\{U, V_d\} < t$. In particular, we prove the existence of unconventional SDW phases for intermediate tilting angles. We use the full interaction, as written in Eq. (1). To deal with the intricate competing orders mentioned in the previous section, we use the functional renormalization group (FRG) technique, which takes an unbiased approach (without any *a priori* guess) to identify the most dominant instability among all possible orders [3, 26–29]. The technical and implementation details of FRG for spin 1/2 fermions on lattice, such as for the Fermi-Hubbard model, have been extensively discussed in the literature (see for example Ref. 30 and references therein) and will not be repeated here. The key ingredients of the FRG calculation are: (1) Derive and solve the renormalization group flows for the generalized four-point vertex between unequal spins, $\mathcal{U}_l^\perp(\mathbf{k}_1, \mathbf{k}_2, \mathbf{k}_3)$, where $\mathbf{k}_{1,2}(\mathbf{k}_{3,4})$ are incoming (outgoing) momenta in the vicinity of the non-interacting Fermi surface, satisfying momentum conservation $\mathbf{k}_1 + \mathbf{k}_2 = \mathbf{k}_3 + \mathbf{k}_4$, and l is the renormalization group flow parameter. The flow of equal spin vertex, $\mathcal{U}_l^\parallel$, is related to that of $\mathcal{U}_l^\perp$ via the spin-rotation symmetry of $\hat{H}$ [27]. (2) For our problem at half filling and with a square Fermi surface, we particularly pay attention to the following interaction channels at each RG step,

$$\begin{aligned}
\mathcal{U}_l^{\mathrm{CDW}}(\mathbf{k}_1, \mathbf{k}_2) &= (2 - \hat{X})\mathcal{U}_l^\perp(\mathbf{k}_1, \mathbf{k}_2, \mathbf{k}_1 + \mathbf{Q}), \\
\mathcal{U}_l^{\mathrm{SDW}}(\mathbf{k}_1, \mathbf{k}_2) &= -\hat{X}\mathcal{U}_l^\perp(\mathbf{k}_1, \mathbf{k}_2, \mathbf{k}_1 + \mathbf{Q}), \\
\mathcal{U}_l^{\mathrm{BCS}}(\mathbf{k}_1, \mathbf{k}_2) &= \mathcal{U}_l^\perp(\mathbf{k}_1, -\mathbf{k}_1, \mathbf{k}_2, -\mathbf{k}_2),
\end{aligned}$$

where the exchange operator $\hat{X}$ interchanges the incoming momenta [27]. (3) Finally we identify the most dominant instability of the Fermi surface from the most divergent eigenvalue of the interaction matrix. The corresponding eigenvector provides information about the orbital symmetry of the incipient order parameter. We note that the Hamiltonian, Eq. (1), is symmetric under lattice inversion. Furthermore, for specific values of ϕ, additional symmetries are realized. For example, for $\theta \neq 0$

and $\phi = 0$, the system has a mirror symmetry with a mirror plane along the x-direction. The order parameters that we discuss in this paper are either even or odd under these symmetries. However, this property alone does not fully characterize the order parameter, two orders of the same parity can be physically distinct, as we will see below.

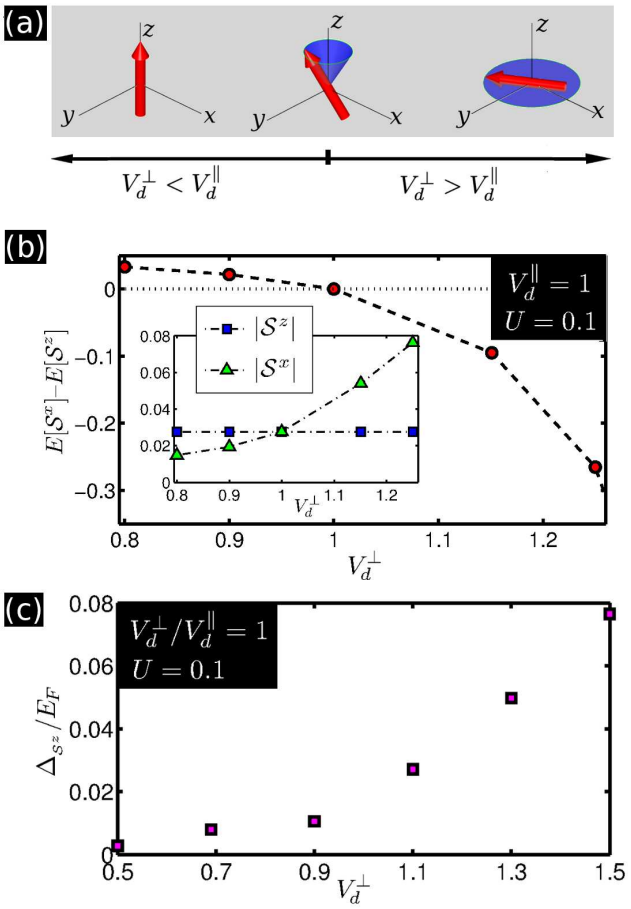

FIG. 3: Mean field results for the SDW$_p$ phase. (a) Preferred direction of the spin polarization vector $\boldsymbol{\mathcal{S}}$ as a function of the ratio $V_d^\parallel/V_d^\perp$. It is along the z-direction for $V_d^\perp < V_d^\parallel$ and lies in the x-y plane for $V_d^\perp > V_d^\parallel$. (b) The energy difference between the mean field states with $\mathcal{S}^z$ and $\mathcal{S}^x$ order. The inset shows the magnitude of the corresponding order parameter. The parameters are $U = 0.1$, $V_d^\parallel = 1.0$, $\theta = 47°$, $\phi = 0$. All energies are in units of t. (c) The mean field energy gap of the SDW$_p$ phase, in units of the Fermi energy, as a function of the inter-spin long-range dipolar interaction $V_d^\perp$ for $\theta = 47°$ and $\phi = 0$. For the SU(2) symmetric case plotted in (c), the energy gaps for different vector polarizations are degenerate.

B. The phase diagram from FRG

The phase diagram summarizing our FRG analysis is shown in Fig. 2. It displays three types of phases: CDW, SDW, and BCS superfluid. We first focus on the case $U < V_d$ in the vicinity of $\phi = 0$ as shown in Fig. 2(a). Consistent with our heuristic argument above, FRG confirms a checkerboard CDW (CDW$_s$) for small θ, and a spin-triplet, p-wave BCS (BCS$_p$) superfluid at large θ. For the intermediate regime, roughly between ϑ_{c1} and ϑ_{c2}, the flow for the SDW channel diverges rapidly, dominating over the CDW and BCS instabilities on either side. The SDW phase shows p-wave orbital symmetry, i.e. the eigenvector of the SDW$_p$ phase (shown in Fig. 2) is essentially of the form $\sin k_y$. This admits an interpretation of SDW$_p$ as a particle-hole analog of triplet superconductivity/superfluidity within Nayak's classification [1] for generalized SDW$_\nu$. The SDW$_p$ phase found here corresponds to the class with $\langle \hat{a}^\dagger_\alpha(\mathbf{k}+\mathbf{Q})\hat{a}_\beta(\mathbf{k})\rangle = \mathbf{S}(\mathbf{k})\cdot\boldsymbol{\sigma}_{\alpha\beta}$, by identifying $\mathbf{S}(\mathbf{k}) \propto \hat{s}\sin k_y$ where $\mathbf{Q} = (\pm\pi, \pm\pi)$. The position space representation implies the checkerboard pattern of hopping amplitudes, $\langle \hat{a}^\dagger_{i,\alpha}\hat{a}_{j,\beta}\rangle$; $\mathbf{r}_j - \mathbf{r}_i = \hat{y}$, depicted in the schematic of Fig. 1(c).

Additional unconventional orders with $\ell \neq 0$ occur in the vicinity of $\phi = 45°$, where the nearest-neighbor interaction along the lattice vectors $\hat{x}$ and $\hat{y}$ is nearly equal. FRG predicts three more phases, CDW$_{s+d}$, SDW$_{s+d}$, and BCS$_{s+d}$, all of which contain a d_{xy}-wave as well as s-wave components. The contributions of the isotropic s-wave, extended s-wave, and d-wave components are inferred by fitting the FRG wavefunctions using function $c_0 + c_1\cos k_x\cos k_y + c_2\sin k_x\sin k_y$, with $\{c_0, c_1, c_2\}$ as fitting parameters. As a general trend, for increasing θ, the magnitude of isotropic s-wave c_0 reduces, while the magnitudes of c_1 and c_2 are comparable and increase. The CDW$_{s+d}$ phase can be viewed as the natural continuation of the CDW$_s$ as c_1 and c_2 become appreciable. The two representative points shown in Fig. 2(a) for the SDW$_{s+d}$ and BCS$_{s+d}$ are fit by $0.05 - 0.16\cos k_x\cos k_y - 0.18\sin k_x\sin k_y$ and $0.01 + 0.23\cos k_x\cos k_y - 0.19\sin k_x\sin k_y$, respectively. Since c_0 is small, the real space modulation pattern for such SDW$_{s+d}$ takes the form of Fig 1(d): atoms delocalize across a plaquette, in the diagonal direction perpendicular to the dipole tilting direction. We note that CDW$_s$ and CDW$_{s+d}$ describe two distinct thermal phases. This is apparent from the low-temperature behavior: The CDW$_s$ phase is fully gapped, whereas the order parameter of the CDW$_{s+d}$ phase has nodal points. This results in a qualitatively different thermal behavior, and therefore these are two distinct phases, even though they have the same parity under the lattice symmetries. In contrast to the triplet BCS$_p$ phase at small ϕ, the BCS$_{s+d}$ phase is a superfluid of singlet Cooper pairs with mixed orbital symmetry, $\ell = 0, 2$.

Next we illustrate how the phase diagram changes as the model approaches the repulsive Fermi-Hubbard model ($U > 0, V_d = 0$). We calculate the FRG flows for increased on-site interaction, $U = 0.5$, while keeping V_d fixed at 0.5. The phase diagram is shown in Fig. 2(b). Since the on-site interaction U favors antiferromagnetism, the SDW$_p$ phase shrinks, while the SDW$_{s+d}$ phase extends to cover a broader region, in-

cluding that previously occupied by BCS_{s+d}. Note that the d-wave component of SDW, even though diminished, is always present since the dipole interaction is kept finite. When U is further increased such that $U \gg V_d$, only the isotropic component (c_0) will survive, indicating the SDW_{s+d} crosses over to SDW_s, the conventional antiferromagnetic ordering of spins in Fig. 1(a).

C. Self-consistent mean field analysis

To corroborate the FRG prediction of the unconventional spin density waves, we use self-consistent mean field theory. For a square lattice of finite size $N \times N$, we impose periodic boundary conditions and retain the dipole interactions up to a distance of 12 lattice constants. We define the various normal and anomalous averages [31], $\rho_{i,\sigma,j,\sigma'} = \langle \hat{a}^\dagger_{j,\sigma'} \hat{a}_{i,\sigma} \rangle$ and $m_{i,\sigma,j,\sigma'} = \langle \hat{a}_{i,\sigma} \hat{a}_{j,\sigma'} \rangle$. The corresponding mean field Hamiltonian is solved self-consistently by starting from an initial guess of the generalized density matrix, and iterating until desired convergence is reached. At each step the chemical potential is tuned to maintain half filling. The results are checked to be size-independent by varying $N > 24$. In Fig. 3, N is set to 28. Although mean field results are only suggestive, they provide an independent confirmation of the FRG results and unveil the real space patterns of $\boldsymbol{\mathcal{S}}$ directly in the SDW_ν phases. They can also be used to investigate the direction of $\boldsymbol{\mathcal{S}}$ for the generalized model with $V_d^\perp(\hat{d}) \neq V_d^\parallel(\hat{d})$. We search for unconventional SDW phases with homogeneous spin density, $n_{i,\sigma} = 1/2$. In and around the SDW_p region predicted by FRG, we indeed find solutions with order parameter $\mathcal{S}^\eta = \sum_{\alpha\beta} \langle \hat{a}^\dagger_{i,\alpha} \hat{\sigma}^\eta_{\alpha\beta} \hat{a}_{j,\beta} \rangle$, $\mathbf{r}_j - \mathbf{r}_i = \hat{y}$. Further, the mean field energy for $\mathcal{S}^x$ order is identical to that for $\mathcal{S}^y$ and $\mathcal{S}^z$, due to the SU(2) symmetry of $\hat{H}$ imposed by $V_d^\perp(\hat{d}) = V_d^\parallel(\hat{d})$. This degeneracy is lifted for $V_d^\perp(\hat{d}) \neq V_d^\parallel(\hat{d})$. In Fig. 3, we compare the mean-field energies of the SDW_p solution with order parameter $\mathcal{S}^z$ and $\mathcal{S}^x$. The $z(x)$- polarized order $\mathcal{S}^z$ ($\mathcal{S}^x$) is energetically favored for $V_d^\parallel > V_d^\perp$ ($V_d^\parallel < V_d^\perp$). However, the degeneracy between $\mathcal{S}^x$ and $\mathcal{S}^y$ remains. The mean field results support our interpretation of the SDW_p order as schematically shown in Fig. 1(c). A similar analysis can be performed for the SDW_{s+d} phase.

IV. CONCLUSION

In conclusion, we provided theoretical evidence for the emergence of unconventional spin density wave orders, SDW_p and SDW_{s+d}, along with other exotic phases with non-zero angular momentum, within ultra-cold spin-1/2 dipolar fermions on the square lattice. These phases occupy a sizable region of the phase diagram mapped out via the functional renormalization group approach. Furthermore, the self-consistent mean field estimation for the energy gaps of SDW_p, shown in Fig. 3(c), indicates a critical temperature $T_c \sim 0.08 T_F$ for $V_d/t = 1.5$. Considering the currently reported temperature of degenerate dysprosium $T \approx 0.2 T_F$ [4], this suggests experimental accessibility of these emergent phases in the near future. Our study shows that the dipolar Fermi system is an intriguing test bed for exotic many-body effects.

Acknowledgments

We thank Benjamin Lev for invaluable discussions. SB and EZ are supported by AFOSR, NIST, and NSF. LM acknowledges support from the Landesexzellenzinitiative Hamburg, which is financed by the Science and Research Foundation Hamburg and supported by the Joachim Herz Stiftung, and from the Deutsche Forschungsgemeinschaft under SFB 925. SWT acknowledges support from NSF under grant DMR-0847801 and from the UC-Lab FRP under award number 09-LR-05-118602.

[1] C. Nayak, Phys. Rev. B **62**, 4880 (2000).
[2] A. J. Leggett, Rev. Mod. Phys. **47**, 331414 (1975).
[3] S. G. Bhongale, L. Mathey, S. -W. Tsai, C. W. Clark, and E. Zhao, Phys. Rev. Lett. **108**, 145301(2012).
[4] M. Lu, N. Q. Burdick, and B. L. Lev, Phys. Rev. Lett. **108**, 215301 (2012).
[5] K. K. Ni, S. Ospelkaus, M. G. H. de Miranda, B. Pe'er, B. Neyenhuis, J. J. Zirbel, S. Kotochigova, P. S. Julienne, D. S. Jin, and J. Ye, Science **322**, 231 (2008).
[6] A. Chotia et al., Phys. Rev. Lett. **108**, 080405 (2012).
[7] C. H. Wu, J. W. Park, P. Ahmadi, S. Will, and M. W. Zwierlein, arXiv:1206.5023.
[8] Y. Yamaguchi, T. Sogo, T. Ito, and T. Miyakawa, Phys. Rev. A **82**, 013643 (2010).
[9] K. Mikelsons and J. K. Freericks, Phys. Rev. A **83**, 043609 (2011).
[10] M. M. Parish and F. M. Marchetti, Phys. Rev. Lett. **108**, 145304 (2012)
[11] A. L. Gadsbolle and G. M. Bruun, arXiv:1206.4974.
[12] M. A. Baranov, L. Dobrek, and M. Lewenstein, Phys. Rev. Lett. **92**, 250403 (2004).
[13] M. A. Baranov, M. S. Mar'enko, V. S. Rychkov, and G. V. Shlyapnikov, Phys. Rev. A **66**, 013606 (2002).
[14] G. M. Bruun and E. Taylor, Phys. Rev. Lett. **101**, 245301 (2008).
[15] N. R. Cooper and G. V. Shlyapnikov, Phys. Rev. Lett. **103**, 155302 (2009).
[16] C. Zhao,L. Jiang, L. Xunxu, W. M. Liw, X. Zou, and H. Pu, Phys. Rev. A **81**, 063642 (2010).
[17] B. M. Fregoso, K. Sun, E. Fradkin, B. L. Lev, New Journal of Physics **11**, 103003 (2009).
[18] J. Quintanilla, S. T. Carr, and J. J. Betouras, Phys. Rev.

A **79**, 031601(R) (2009).
[19] K. Sun, C. Wu, and S. D. Sarma, Phys. Rev. B **82** 075105 (2010).
[20] A. Micheli, G. K. Brennen, and P. Zoller, Nature Physics **2**, 341 (2006).
[21] A. V. Gorshkov, S. R. Manmana, G. Chen, J. Ye, E. Demler, M. D. Lukin, and A. M. Rey, Phys. Rev. Lett. **107**, 115301 (2011).
[22] L. He and W. Hofstetter, Phys. Rev. A **83**, 053629 (2011).
[23] B. M. Fregoso and E. Fradkin, Phys. Rev. Lett. **103**, 205301 (2009).
[24] T. Sogo, M. Urban, P. Schuck, and T. Miyakawa, Phys. Rev. A 85, 031601(R) (2012).
[25] Y. Li and C. Wu, Phys. Rev. B **85**, 205126 (2012).
[26] R. Shankar, Rev. Mod. Phys. **66**, 129 (1994).
[27] D. Zanchi and H. J. Schulz, Phys. Rev. B **61**,13609 (2000).
[28] L. Mathey, S. -W. Tsai, and A. H. Castro Neto, Phys. Rev. Lett. **97**, 030601 (2006);
[29] L. Mathey, S. -W .Tsai, and A. H. Castro Neto, Phys. Rev. B **75**, 174516 (2007).
[30] W. Metzner, M. Salmhofer, C. Honerkamp, V. Meden, and K. Schoenhammer, Rev. Mod. Phys. **84**, 299 (2012).
[31] Blaizot, J. -P. & Ripka, G., *Quantum Theory of Finite Systems*, MIT Press, Cambridge MA (1985).